

Superconductivity above the lowest Earth temperature in pressurized sulfur hydride

Antonio Bianconi^{1,2,3}, Thomas Jarlborg^{1,4}

¹ RICMASS, Rome International Center for Materials Science Superstripes, Via dei Sabelli 119A, 00185 Rome, Italy

² Institute of Crystallography, Consiglio Nazionale delle Ricerche, via Salaria, 00015 Monterotondo, Italy

³ INSTM, Consorzio Interuniversitario Nazionale per la Scienza e Tecnologia dei Materiali, Rome Udr, Italy

⁴ DPMC, University of Geneva, 24 Quai Ernest-Ansermet, CH-1211 Geneva 4, Switzerland

A recent experiment has shown a macroscopic quantum coherent condensate at 203 K, about 19 degrees above the coldest temperature recorded on the Earth, 184 K (-89.2 C, -128.6 F) in pressurized sulfur hydride. This discovery is relevant not only in material science and condensed matter but also in other fields ranging from quantum computing to quantum physics of living matter. It has given the start to a gold rush looking for other macroscopic quantum coherent condensates in hydrides at the temperature range of living matter $200 < T_c < 400K$. We present here a review of the experimental results and the theoretical works and we discuss the Fermiology of H_3S focusing on Lifshitz transitions as a function of pressure. We discuss the possible role of the *shape resonance* near a *neck disrupting* Lifshitz transition, in the Bianconi-Perali Valletta (BPV) theory, for rising the critical temperature in a multigap superconductor, as the Feshbach resonance rises the critical temperature in Fermionic ultracold gases

PACS numbers: 74.10.+v, 74.70.Ad, 74.20.-z

In March 2014 Mikhail Eremets and his collaborators recorded in their logbook the first evidence of high temperature superconductivity in the high pressure metallic phase of H_2S [1, 2] as he reported at the Superstripes 2015 conference [3]. Independently, at the same time, Yinwei Li et al. [4] published the theoretical prediction that the metallic phase of H_2S at high pressure should be a stable superconductor with high T_c . In the fall 2014 the work of Duan et al. [5] predicted high temperature superconductivity in metallic H_3S , formed by pressure induced disproportionation of $2(H_2S) + H_2$ at around 100 GPa.

The record of superconductivity at 190 K in pressurized H_2S was reported in December 2014 by evidence of zero resistivity [1] followed by Meissner effect in June

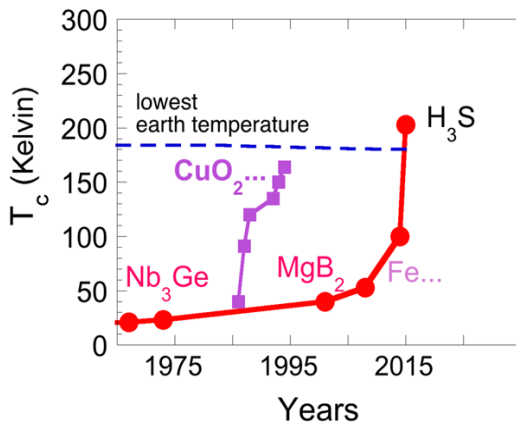


FIG. 1: (Color online) Records for the highest superconducting critical temperature found in: cuprates (1994), made of CuO_2 layers intercalated by spacer layers, in MgB_2 (2001), in iron based superconductors (2008), made of Fe layers intercalated by spacer layers, followed in 2014 by 100K superconductivity in FeSe films on doped $SrTiO_3$.

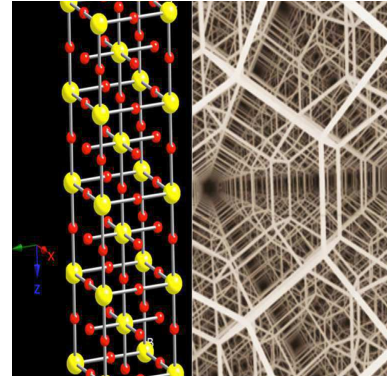


FIG. 2: (Color online) The left panel shows the high pressure $Im\bar{3}m$ phase of H_3S . Yellow large spheres indicate sulfur atoms and the red small spheres indicate hydrogen atoms. The $Im\bar{3}m$ is formed by two intertwined set of chains made of S-H-S covalent bonds. The right panel shows a picture of the complex 3D space filling made of truncated cubic tiling at the border line between crystals and quasicrystals.

2015 [3] with a maximum T_c onset of 203 K [2] establishing a record for the superconductor with the highest critical temperature. The previous $T_c=164K$ record was held by doped $HgBa_2Ca_2Cu_3O_8$, at a pressure of 15 GPa [6] as shown in Fig. 1. The theoretical works on the structure prediction have been performed using the USPEX algorithm, Universal Structure Predictor Evolutionary Xtallography, [7] already applied to predict superconductivity in LiH_n [8].

High temperature superconductivity in pressurized H_3S has been recently confirmed and the crystal structure has been measured [9, 10]. H_3S crystallizes with the $Im\bar{3}m$ lattice symmetry, as predicted [5]. This structure (see Fig. 2) is at the border line between crystals and quasicrystals [11, 12]. In the expected low pressure $R\bar{3}m$

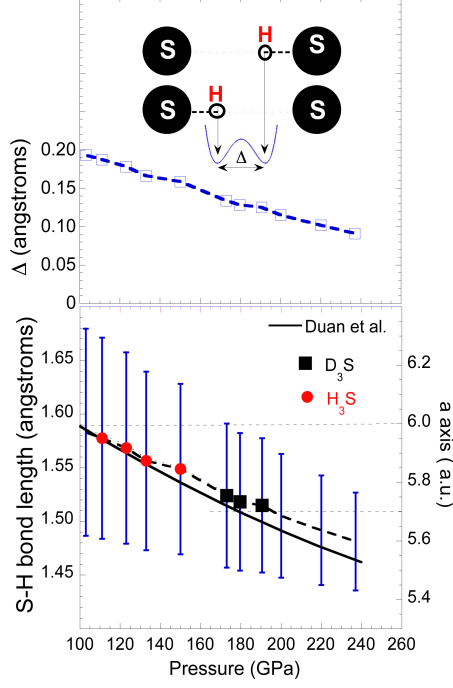


FIG. 3: (Color online) Upper panel: the spatial separation Δ between the minima of the expected double well potential for hydrogen along the S-S direction in H_3S typical of the S-H hydrogen bond. Lower panel: the S-H bond distances in H_3S (filled red dots) and D_3S (black squares) as a function of pressure[9] and the prediction of Duan et al. (black solid line)[5]. The error bars show the amplitude of the expected fluctuations of the S-H bond calculated by the difference between the two minima of the a double well potential for the H atoms.

phase H_3S shows long and short hydrogen S-H bonds[5], like in ice crystals, with a double potential well as shown in Fig. 3. The separation Δ between the minima of the double well decreases with pressure, so the amplitude of H zero point motion decreases with increasing pressure. The experimental structure[9] shows minor divergence from theory predictions[5] (see Fig. 3). The system is quite inhomogeneous with broad line-shapes of diffraction profiles becoming sharper at high pressure. Moreover the system shows a large increase of the critical temperature by annealing the sample temperature at 300K, see Fig. 4, like in oxygen doped cuprates [13]. Therefore an intrinsic optimum inhomogeneity favors superconductivity, like in A15 compounds[14], cuprates[15, 16], diborides[17] and iron chalcogenides[18].

In the past decades the search for new high temperature superconductors has provided evidence for a large variety of different materials with high T_c . A binary intermetallic Nb_3Ge , with A15 crystalline structure, has hold the record of $T_c=23K$ for many years[14]. This record was exceeded in 1986 by Bednorz and Muller with the discovery[19] of 35K superconductivity in doped La_2CuO_4 , which was followed by the discovery of many superconducting cuprate perovskites made

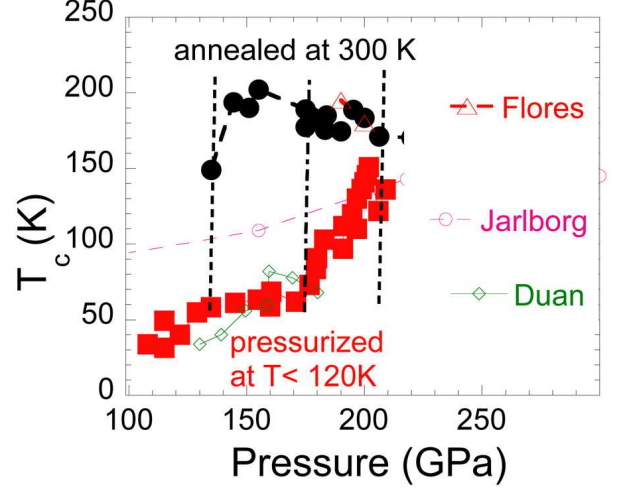


FIG. 4: (Color online) The critical temperature of H_3S samples pressurized at low temperature (filled red squares) and annealed at room temperature (filled black dots) [2, 9]. The experiment shows a metastable phase in the pressure range between 140 and 205 GPa where the critical temperature depends on different thermal and pressure treatments. Calculated critical temperature by Duan et al.[5], (open diamonds) Jarlborg et al.[58], (open red circles) Flores et al.[68] (open red triangles).

of CuO_2 atomic layers intercalated by a large variety of spacer layers. The record of $T_c=160$ K critical temperature in cuprates was achieved by optimization of mainly three physical parameters:

- a) the misfit strain [20–23] between the CuO_2 layers and different spacer layers;
- b) the amount of added dopants in the spacer layers (oxygen interstitials) [13, 15, 16];
- c) the application of an external pressure, 15 GPa, in $HgBa_2Ca_2Cu_3O_8$ ($Hg1223$) [6].

In 2001 the record for intermetallics was obtained by Akimitsu and his colleagues measuring transport properties in an intermetallic compound made of light elements MgB_2 , known since 1953 and already in the market, finding the superconducting transition at $T_c = 40K$ [24].

In 2008 Hosono and his colleagues made the accidental discovery of a new kind of superconducting transition metal oxide, $LaAsFeO$, a layered compound doped with fluorine, with $T_c = 26$ K [25] which has triggered the iron age of iron based superconductors with the record of $T_c = 100$ K in $FeSe$ monoatomic films deposited on doped $SrTiO_3$ [26].

Eremets et al. followed for many years the research direction for high temperature superconductivity at high pressure[27–30]. They discovered that metallic silane becomes superconductor with $T_c = 17$ K at 96 GPa[31] and recently they have found that PH_3 shows a $T_c = 100$ K at high pressures[32]. Computational materials discovery is now addressed to hydrides considered to be pre-compressed phases of solid hydrogen such as YH_4 and YH_6 [33], tellurium hydrides [34], VH_2 [35], AlH_3 [36],

SbH_4 [37] and polonium hydrides [38]. Superconductivity was predicted in LiH_6 with $T_c = 82$ K at 300 GPa [39], in KH_6 with $T_c = 70$ K at 166 GPa [40], with the computed record of $T_c = 235$ in CaH_6 at 150 GPa [41].

Many years before high temperature superconductivity in pressurized hydrides and hydrogen was proposed by Ashcroft [42–47], Ginzburg [48, 49] and Maksimov [50, 51]. The theoretical predictions of high T_c in solid hydrogen and hydrides at high pressure were based on the search of a system with i) a high energy phonon mediating the pairing, because of the small mass of the hydrogen ion, with ii) a negative dielectric constant [49–51] and iii) at the verge of superfluid-superconductor transition [46], where the transition temperature principally increases through the reduction in the associated Coulomb pseudopotential.

The isotope effect in H_3S [1] provided a direct evidence for the conventional phonon mediated pairing. Therefore theories of unconventional pairing based on exchange of magnetic interactions have been ruled out. From the results in ref. [2], the isotope coefficient as a function of pressure was reported by [52]. Fig. 5 shows the pressure dependent isotope coefficient from data in ref. [9]. The isotope coefficient shows a minimum of $\alpha=0.2$ at 200 GPa, a maximum, $\alpha=1$ at 140 GPa and a second maximum $\alpha=0.3$ around 240 GPa. A similar pressure dependent isotope coefficient has been found in cuprates superconductors as a function of doping [53, 54] with anomalies at Lifshitz transitions [55, 56] of the $L1$ type, *appearing of a new Fermi arc*, or of the $L2$ type, *neck disrupting* [57] (see Fig. 6). Therefore the data in Fig. 5 have been interpreted [52] as indication of the presence of Lifshitz transitions in the pressure range showing high temperature superconductivity. The Lifshitz transitions i.e., the electronic transitions in the Fermi surface topology of H_3S as function of pressure in the range from 80 GPa to 250 GPa have been identified by band structure calculations in ref. [52, 58], which have been confirmed [59]. The giant effect of sample annealing in the range 140–200 GPa in H_3S due to the predicted arrested phase separation near Lifshitz transitions [60, 61] as for cuprates where intrinsic phase separation and inhomogeneity are key features of high temperature superconductivity [15, 16, 62].

The superconducting temperature in sulfur hydride was interpreted by a series of theoretical papers using the standard BCS approximations. First, the *dirty limit approximation* reducing multiple bands, crossing the chemical potential, to a simplified metal with a single effective band. Second, the *Migdal approximation* considering the chemical potential very far from band edges so that the electronic and ionic degrees of freedom can be rigorously separated in agreement with the Born-Oppenheimer approximation. The superconducting temperature was predicted by employing the Allen-Dynes modified McMillan formula [5, 63], the Migdal Eliashberg formula [64–67], and the more advanced density-functional theory SCDF [68, 69]. The super-

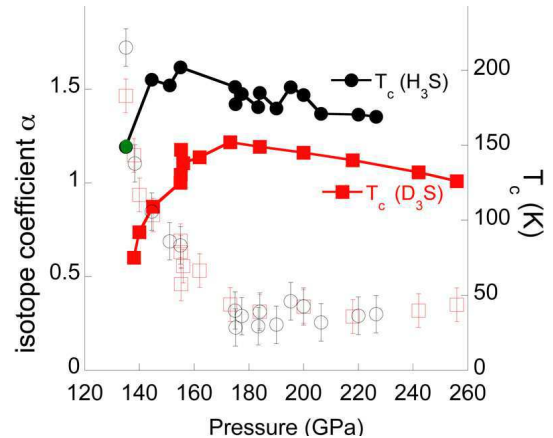


FIG. 5: (Color online) The isotope coefficient as a function of pressure, (open black circles) calculated from the critical temperature T_c of H_3S (black solid dots) and the interpolated T_c of D_3S at the same pressure. The isotope coefficient, (open red squares) calculated from the critical temperature T_c of D_3S (red solid squares) and the interpolated T_c of H_3S at the same pressure from the data reported by Drozdov et al. [2] and Einaga et al. [9].

conducting condensate has been described in the frame of isotropic pairing with a single gap Δ_0 in the BCS regime $\Delta_0/E_F \ll 1$ and in the Migdal approximation $\omega_0/E_F \ll 1$, where the Fermi energy E_F is the energy separation between the chemical potential and the bottom of valence bands at -25 eV. The pre-factor, ω_0 , in the BCS formulas is very high of the order of 100–150 meV due to a high energy phonon branch formed by hydrogen ions dynamics [65, 68, 69]. However both the electron-phonon coupling and the total density of states (DOS) are not very large. The phonon energy of 100–150 meV giving the energy cut-off of the pairing interaction in H_3S should be compared with the 70 meV phonon energy of i) the half-breathing Cu-O-Cu mode, mediating the pairing in cuprates [70], and i) the e_{2g} mode in magnesium diboride [71] that show moderate energy softening due to electron-phonon interaction. The moderate softening there is due to the fact that these phonons interact only with small portions of electrons on the Fermi surface: the Fermi arc around the antinodal $(\pi, 0)$ point in cuprates, and the small tubular σ Fermi surface in MgB_2 .

Starting from the evidence of Lifshitz transitions the Bianconi, Perali, Valletta (BPV) theory [57, 72] was proposed [52, 58] to describe high temperature superconductivity in H_3S . The BPV theory considers high temperature superconductivity made of multiple condensates. The optimum critical temperature is predicted for a first condensate in the BCS regime and the second one in the BCS-BEC crossover near a Lifshitz transition of the *neck disrupting* type as shown in Fig. 6.

The BPV theory is based on the general theory of superconductivity [73–75] with no ad-hoc BCS approximations. It was proposed in 1996 for cuprates [53], was verified in 2001 in diborides [76], and in 2009 for iron based

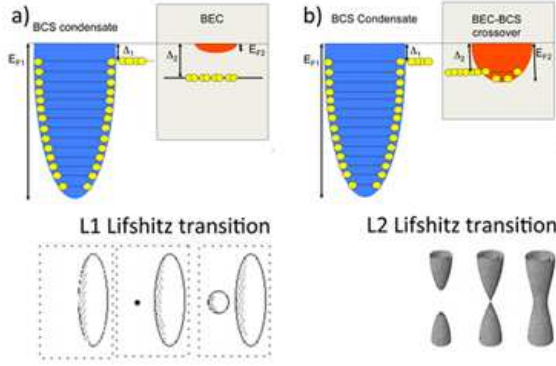


FIG. 6: (Color online) Pictorial view for the shape resonance described by the BPV theory for two condensates superconductor. The first case where T_c is suppressed is shown in panel a) with the first condensate in the BCS regime and the second condensate in the BEC regime (upper panel) at the Lifshitz transition [52], L1 type, for the *appearing of a new Fermi surface spot* (left lower panel). The second case where T_c is maximum is shown in panel b) with the first condensate in the BCS regime and the second condensate in the BCS-BEC crossover regime (upper panel) realized at the Lifshitz transition [52], L2, for *neck disrupting Fermi surface* (right lower panel).

superconductors [77, 78], where the highest T_c at a *neck disrupting* Lifshitz transition was observed by high resolution ARPES, experiments [79–82]. Different condensates are formed in different Fermi surfaces with different symmetry and different Fermi energies E_{nF} . The shape resonance provides a key quantum interaction increasing the critical temperature, like Feshbach resonance in ultracold gases. The shape resonance is a contact interaction not included in the standard Eliashberg theory. It is an exchange interaction between first pairs in a first BCS condensate and second pairs in a second condensate in the BCS-BEC crossover regime (see Fig. 6). It belongs to the class of Fano-Feshbach resonances widely investigated theoretically and experimentally in ultracold fermionic gases [83–85] where the Feshbach resonance is the only pairing mechanism giving high temperature superconductivity with $k_B T_c / E_F = 0.2$. Therefore information on the Fermi surfaces are essential for the BPV superconductors made of multiples condensates in multiple Fermi surfaces. The Fermi surface of H_3S at 200 GPa, i.e., for $a = 5.6$ a.u., is shown in Fig. 7. It is formed by 5 different Fermi surfaces calculated in the bcc Brillouin zone (bcc BZ) like in YB_6 [33].

The large Fermi surface (FS) No.2 coexists with the cubic-like FS No.1, and three small closed FS at Γ point No.3,4,5. The band dispersion shown in Fig. 8 has been calculated in the simple cubic Brillouin zone (sc BZ), where the simple cubic unit cell contains 8 sites, since it grabs key features of the electronic structure [52, 58]. The use of sc BZ in Fig. 8 is widely used for A15 superconductors. In fact here H ions on the limits of the simple cubic cell forms linear chains, as the transition metals

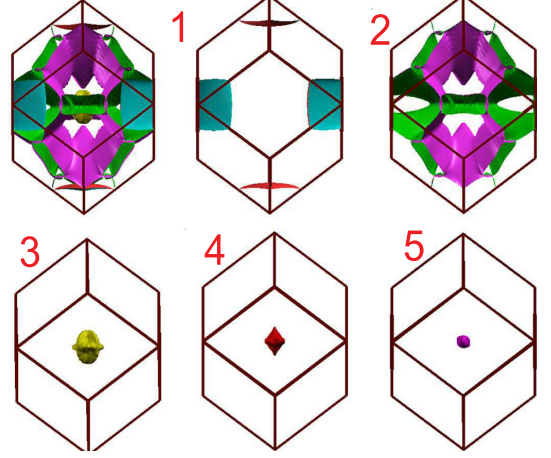


FIG. 7: (Color online) The Fermi surface for H_3S with $Im\bar{3}m$ structure for the lattice parameter $a = 5.6$ a.u. at 200 GPa shown on the top left side of the figure. The Fermi surface is formed by 5 different Fermi surfaces from 1 to 5. The first and second large Fermi surfaces coexist with 3 small Fermi surface pockets (No.3, No.4, No.5) centered at the Γ -point (FS calculations made by Yinwei Li [33]).

form linear chains in A15 compounds, and the S sites form a bcc lattice. The band dispersion of the second band at about $2/3$ of the Γ -M direction shows a maximum above the Fermi level for $a = 5.6$ a.u. as reported in Fig. 8. The partial density of states only for the bands crossing the Fermi energy is shown in the panel on the left side of Fig. 8. The density of states associated with the No.2 band shows the highest contribution to the total density of states (DOS). For $a = 5.6$ a.u. lattice parameter, we see that the van Hove singularity, associated with the derivative peak at the high energy side of the narrow DOS peak, is above the chemical potential, at the same energy position as the top of the band dispersion at $2/3$ of the Γ -M direction. The discontinuity of the DOS indicates a topology change of a portion of the Fermi surface from a 3D topology to 2D topology. The 2D portions of the Fermi surface appear in the Fermi surface No.2 in Fig. 7 as tubular necks, in the HNH direction of the bcc BZ, connecting the large petals of the No.2 Fermi surface. These tubular necks give the flat energy dependence at the peak of the DOS maximum near the chemical potential. The three small Fermi surface pockets (No.3, No.4, No.5) centered at the Γ -point in Fig. 7 correspond with the three tops at the Γ -point of three rapidly dispersing bands in Fig. 8. These bands give a small contribution to the total density of states but are very sensitive to pressure changes.

The Lifshitz transitions driven by pressure are shown in Fig. 8 and in Fig. 9. The tops of the dispersing bands at the Γ -point in Fig. 8 are pushed up by pressure.

The L1 Lifshitz transitions for a *new appearing Fermi surface spot* occurs where the bands at the Γ -point cross the chemical potential. The side view pictures of all

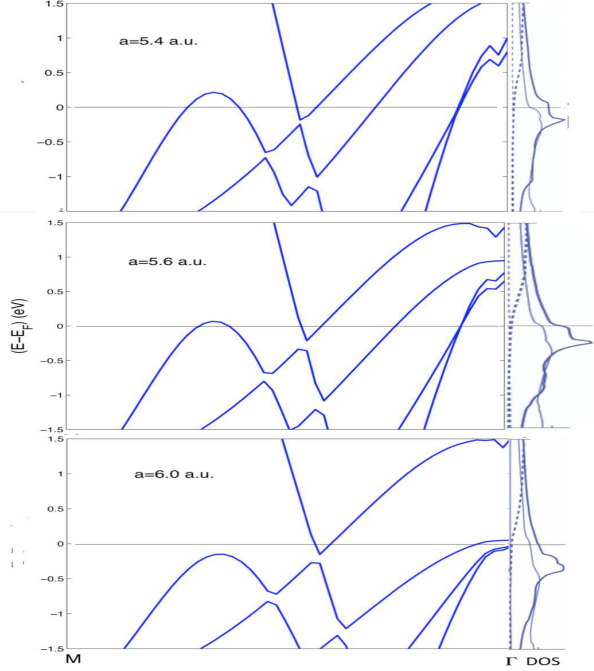


FIG. 8: (Color online) The band structure along $M-\Gamma$ points of the simple cubic double cell Brillouin zone (sc BZ) for H_3S at different the lattice parameters in the range between 5.4 a.u. and 6. a.u. The figure shows the shift of the top of a band at about $2/3$ in the $M-\Gamma$ direction from low pressure ($a=6.0$) to high pressure ($a=5.4$) and and at 200 GPa, where it is crossing the chemical potential. The top of this band corresponds to a saddle point on the band dispersion. This crossing point is associated with a neck disrupting Lifshitz transition in the Fermi surface No.2. Moreover it is associated with the divergent derivative of the partial density of states (DOS) of band No.2 on the high energy side of the sharp DOS peak near the Fermi level. The partial density of states for each band is shown in the left side of the figure.

Fermi surfaces in Fig. 9 show that the small red closed Fermi surfaces at Γ are not present for $a=6.0$ a.u. while they appear at high pressure as a red sphere, as shown for $a=5.4$ a.u.. The energy shift of the tops of the hole-like bands No. 3, No. 4 at the Γ point are shown in Fig. 10. The $L1$ Lifshitz transitions for the appearing of the new Fermi surface spots at Γ occurs around 100 GPa, as shown in Fig. 10 at the onset of the observed superconducting phase where T_c is close to zero as predicted by the BPV theory .

The $L2$ Lifshitz transition for *neck disrupting* (see Fig. 6) driven by pressure is due to the top of the band at $2/3$ in the Γ - M direction in Fig. 8 moving from below to above the chemical potential with increasing pressure. The top view of Fig. 9 shows the formation of the tubular 2D necks missing at $a=6.0$ a.u. appearing for $a < 5.7$ a.u.. These necks connect the large Fermi surface petals as seen in the top view of Fig. 9. The energy of the top of the band at about $2/3$ of the Γ - M direction corresponds with the energy of the discontinuity in the high energy

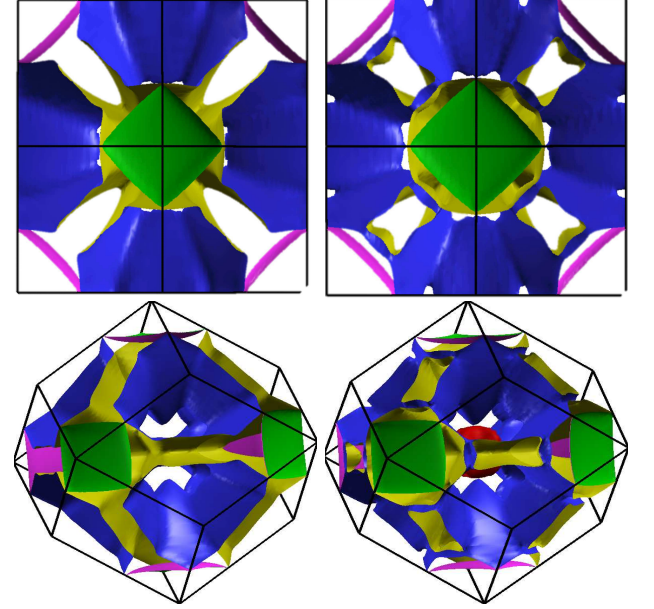


FIG. 9: (Color online) The two top (bottom) color pictures show the top (side) view of the Fermi surface of H_3S at low ($a=6.0$ a.u.) (left panel) and high ($a=5.4$ a.u.) (right panel) pressure. The green and pink surfaces are portions of the Fermi surface No. 1. The blue and yellow surfaces are portions of the Fermi surface No. 2. The tubular necks in the Fermi surface connecting the large petals of the Fermi surface No.2 appear in the high pressure ($a=5.4$ a.u.) picture. This shows the Fermi surface topology change for $a \leq 5.7$ a.u. due to the Lifshitz transition for a *Fermi surface neck disrupting, L2 type*. The red small Fermi surface pockets No.3, No.4, No.5 centered at the Γ -point appear for $a < 6.0$ a.u. with the change of the Fermi surface topology called Lifshitz transition $L1$ for *new appearing Fermi surface spot* (FS calculations made by Antonio Sanna [68]).

side of the narrow DOS peak near the chemical potential indicating the van Hove singularity. The appearing of the 2D necks, by increasing pressure, Fig. 10. occurs in the pressure range, around 180-200 GPa, where the high critical temperature is maximum and the isotope coefficient is minimum as predicted by the BPV theory [57, 72])

The Migdal approximation breakdown for electrons at the Lifshitz transitions and they enter in the BEC or BCS-BEC crossover. While Eliashberg theory breakdown, the BPV theory describes the system by solving both the gap and the density equation and by including the chemical potential shifts in the superconducting phase. The shape resonance emerges between few pairs in BEC or BCS-BEC crossover and all other pairs in BCS regime. The hydrogen zero point motion gives [58] a relevant renormalization of the energy levels like electronic correlation and the related energy fluctuations[58], as in diborides [17, 86, 87], extend the energy range of shape resonances.

In conclusion superconducting H_3S has a complex crystal structure at the borderline with quasicrystals. The

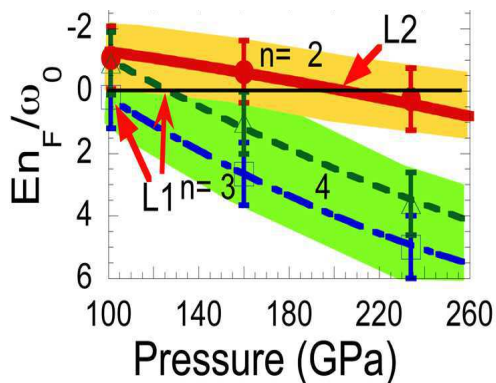


FIG. 10: (Color online) Blue and green dashed lines show the pressure dependence of the Fermi energy for the hole-like bands, No. 3 and No. 4, crossing the chemical potential at the $L1$ Lifshitz transition, see Fig. 6. The red solid line shows the Fermi energy at the saddle point, at about $2/3$ of the $\Gamma - M$ distance, crossing the chemical potential at the $L2$ Lifshitz transition, see Fig. 6. The Fermi energy is divided by the effective pairing energy cut off (taken here to be 150 meV) due to phonon frequency and zero point motion energy fluctuations [58] as in diborides [17, 86, 87]. The errors bars and the colored region indicates the energy fluctuation range of the band edges.

hydrogen bond plays a key role with large H atomic fluctuations. The system shows intrinsic inhomogeneity with segregation of sulfur moreover it shows lattice instabil-

ity been sensitive to thermal annealing processes Fig. 4, like in oxygen doped cuprates where T_c is increased by thermal annealing and under illumination [13]. The high frequency phonon mode is a key prefactor but also other factors like an anomalous dielectric constant and heterogeneity should cooperate to drive superconductivity to high temperature. The zero-point motion of the light H-atoms induces strong electronic renormalization [58]. H_3S is a multiband superconductor with five different Fermi surfaces with first condensates in the BCS regime coexist with second condensates in the BCS-BEC crossover regime (located on small Fermi surface spots with small Fermi energy). The shape resonance near a $L2$ Lifshitz transition, neglected in the Eliashberg theory, described by the BPV theory including both i) corrections of the chemical potential due to pairing, and ii) the configuration interaction between different condensates is expected to play a key role in the road map for theory driven search of room temperature superconductors.

Acknowledgments

We thanks Mikhail Erements, Ryotaro Arita, Emanuele Cappelluti and L. Ortenzi for discussions, and Antonio Sanna and Yinwei Li for their Fermi surface color plots. We acknowledge financial support of superstripes institute.

-
- [1] Drozdov A.P., Erements M.I., Troyan I.A., Preprint arXiv:1412.0460 (1 December 2014)
 - [2] Drozdov A.P., Erements M.I., Troyan I.A., Ksenofontov V., Shylin S.I., Nature **525** (2015) 73
 - [3] Erements M.I. in Bianconi A. ed. Superstripes 2015 (Superstripes Press, Rome) 2015, p. 286 Isbn: 9788866830382.
 - [4] Li Yinwei, Hao J., Liu H., Li Y., Ma Y., The Journal of Chemical Physics **140** (2014) 174712
 - [5] Duan D., Liu Y., Tian F., *et al.*, Sci. Rep. **4** (2014) 6968
 - [6] Gao L. *et al.* Physical Review B **50** (1994) 4260
 - [7] Lyakhov A. O., Oganov A. R. Stokes H.T., Zhu Q. Comput. Phys. Commun. **184** (2013) 1172
 - [8] Zurek E., Hoffmann R., Ashcroft N. W., Oganov A. R., Lyakhov A. O. Proceedings of the National Academy of Sciences **106**(2009)17640
 - [9] Einaga M., *et al.* Preprint arXiv:1509.03156 (2015)
 - [10] Li Y., *et al.* Preprint arXiv:1508.03900 (2015)
 - [11] Steurer W., Deloudiry S., Crystallography of Quasicrystals: Concepts, Methods and Structures Springer series in material science **126** (2009) 384
 - [12] Ramsden S. J. , Robins V. , Hyde S. T. , Acta Crystallographica Section A: Foundations of Crystallography **65** (2009) 81
 - [13] Poccia N., Fratini M., Ricci A., Campi G., Barba L. *et al.* Nature materials **10** (2011) 733
 - [14] Testardi, L.R., Review of Modern Physics **47** (1975) 637
 - [15] Campi G. *et al.*, Nature **525** (2015) 359
 - [16] Poccia, N., *et al.* Proceedings of the National Academy of Sciences **109** (2012) 15685
 - [17] Campi G., *et al.* The European Physical Journal B - Condensed Matter and Complex Systems, **52** (2006) 15
 - [18] Ricci, A. *et al.* Phys. Rev. B **84** (2011) 060511
 - [19] Bednorz J. G., Muller K. A. Reviews of Modern Physics **60** (1988) 585
 - [20] Bianconi A., Bianconi G., Caprara S., Di Castro D., Oyanagi H., Saini N.L. Journal of Physics: Condensed Matter **12** (2000) 10655
 - [21] Bianconi, A., Agrestini, S., Bianconi G., Di Castro D., Saini N.L., Journal of alloys and compounds **317** (2001) 537
 - [22] Agrestini S., Saini N.L., Bianconi G., Bianconi A. Journal of Physics A: Mathematical and General **36** (2003) 9133
 - [23] Bianconi, A., *et al.*, International Journal of Modern Physics B **14** (2000) 3342
 - [24] Nagamatsu, J., Nakagawa, N., Muranaka, T., Zenitani, Y., Akimitsu, J., Nature **410** (2001) 63
 - [25] Kamihara, Y., Watanabe, T., Hirano, M., Hosono, H., J. Am. Chem. Soc. **130** (2008) 3296
 - [26] Ge J.-F. *et al.* Nature Materials **14** (2014) 285
 - [27] Amaya K., Shimizu K., Takeshita N., *et al.* The Review of High Pressure Science and Technology **7** (1998) 688
 - [28] Amaya K., Shimizu K., Erements M. I., Int. J. Mod. Phys.

- B **13** (1999) 3623.
- [29] Lorenz B., Chu C. W., In: Narlikar, A. (Ed.) *Frontiers in Superconducting Materials*. Springer Berlin Heidelberg (2005) Ch. 12, pp. 459-497.
- [30] Eremets M. I., Shimizu K., Kobayashi T. C., Amaya K., *Journal of Physics: Condensed Matter* **10** (1998) 11519
- [31] Eremets M. I., Trojan I. A., Medvedev S. A., Tse J. S., Yao Y., *Science* **319** (2008) 1506-1509.
- [32] Drozdov A. P., Eremets M. I., Troyan I. A., preprint arXiv:1508.06224 Aug. 2015.
- [33] Li Y., Hao J., Liu H., Tse J. S., Wang Y., Ma Y., *Scientific Reports* **5** (2015) 9948
- [34] Zhong X., et al. preprint arXiv:1503.00396 (March 2015)
- [35] Chen C., Tian F., Duan D., et al. *The Journal of Chemical Physics*, **140** (2014) 114703
- [36] Hou P., Zhao X., Tian F., Li D., Duan D., Zhao Z., Chu B., Liu B., Cui T., *RSC Adv.* **5** (2015) 5096
- [37] Ma Y., et al. preprint arXiv:1506.03889 (2015)
- [38] Liu Y., et al. preprint arxiv: 1503.08587 (2015)
- [39] Xie Y., Li Q., Oganov A. R., Wang H., *Acta Crystallographica Section C: Structural Chemistry* **70** (2014) 104
- [40] Zhou D., et al. *Phys. Rev. B* **86** (2012) 014118
- [41] Wang H., et al. *Proc. Nat. Acad. Sci. U.S.A.* **109** (2012) 6463
- [42] Ashcroft N. W. *Physical Review Letters* **21** (1968) 1748
- [43] Richardson C. F., Ashcroft N. W. *Phys. Rev. Lett.* **78** (1997) 118
- [44] Ashcroft N. W., *Physical Review Letters* **92** (2004) 187002
- [45] Ashcroft N. W., in Bianconi A. ed. *Symmetry and Heterogeneity in High Temperature Superconductors*, 214, Springer Netherlands (2006)
- [46] Babaev E., Sudbo A., Ashcroft N.W., *Nature* **431** (2004) 666
- [47] Abe K. and Ashcroft N.W., *Phys. Rev. B* **88** (2013) 174110
- [48] Ginzburg V. L., *Sov. Phys. Usp.* **12** (1969) 241
- [49] Ginzburg V. L., Kirzhnits, D. A. *High temperature superconductivity*. Consultants Bureau, Plenum Press, (New York, 1982)
- [50] Maksimov E. G., *Savrasov Solid State Communications* **119** (2001) 569
- [51] Maksimov E. G. and Dolgov O. V. *Physics-Uspekhi* **40** (2007) 933
- [52] Bianconi A., Jarlborg T., *Novel Superconducting Materials* **1** (2015) 37 DOI 10.1515/nsm-2015-0006; Preprint arXiv: 1507.01093 (2015)
- [53] Bianconi A., Valletta A., Perali A., Saini N.L. *Physica C: Superconductivity* **296** (1998) 269
- [54] Perali A., Innocenti D., Valletta A., Bianconi A., *Superconductor Science and Technology* **25** (2012) 124002
- [55] Lifshitz I. M., *Sov. Phys. JETP* **11** (1960) 1130
- [56] Varlamov A. Edorov V., Pantsulaya A., *Advances in Physics* **38** (1989) 469
- [57] Bianconi A., *Journal of Superconductivity* **18** (2005) 625
- [58] Jarlborg T., Bianconi A., preprint arXiv:1509.07451
- [59] Quan Y., Pickett W.E., preprint arXiv:1508.04491 (2015)
- [60] Kugel, K. I. et al. *Phys. Rev. B* **78** (2008) 165124
- [61] Bianconi A., et al. *Supercond. Sci. Technol.* **28** (2015) 024005
- [62] Bianconi A., Di Castro D., Bianconi G., Pifferi A., Saini N.L., Chou F.C., et al. *Physica C: Superconductivity* **341** (2000) 1719
- [63] Duan D., Huang X., Tian F., Li D., Yu H., Liu Y., Ma Y., Liu B., Cui T., *Phys. Rev.B* **91** (2015) 180502
- [64] Papaconstantopoulos D., et al. *Phys. Rev. B* **91** (2015) 184511
- [65] Errea I., et al. *Phys. Rev. Lett.* **114** (2015) 157004
- [66] Durajski A. P., Szczesniak R., Li Y., *Physica C: Superconductivity and its Applications* **515** (2015) 1
- [67] Nicol E.J., Carbotte J.P., *Physical Review B* **91** (2015) 220507
- [68] Flores-Livas J.A., Sanna A., Gross E.K.U., preprint arXiv:1501.06336v1 (2015)
- [69] Akashi R., Kawamura M., Tsuneyuki S., Nomura Y., Arita R., *Phys. Rev. B*, **91** (2015) 224513
- [70] Reznik D., et al., *Nature* **440** (2006) 1170
- [71] Simonelli L., et al. *Physical Review B* **80** (2009) 014520
- [72] Bianconi A., *J. Phys.: Conf. Ser.* **449** (2013) 012002
- [73] Weinberg S., *Progress of Theoretical Physics Supplement* **86** (1986) 43
- [74] Blatt J. M., *Theory of Superconductivity*, Academic Press, New York (1964).
- [75] Leggett A. J., in Pekalski A., Przystawa, R. ed., *Modern Trends in the Theory of Condensed Matter*, Lecture Notes in Physics, 115, Springer-Verlag, Berlin, (1980) p. 13.
- [76] Innocenti D., et al. *Phys. Rev. B* **82** (2010) 184528
- [77] Caivano R. et al. *Superconductor Science and Technology* **22** (2009) 014004
- [78] Bianconi A., *Nature Physics* **9** (2013) 536
- [79] Charnukha A. et al. *Scientific Reports* **5** (2015) 10392
- [80] Kordyuk A. A. *Low Temperature Physics* **41** (2015) 319
- [81] Liu C. et al., *Physical Review B* **84** (2011) 020509
- [82] Borisenko S.V., et al. *Symmetry* **4** (2012) 251
- [83] Chin C., Grimm R., Julien P., Tiesinga E. *Reviews of Modern Physics* **82** (2010) 1225
- [84] Greiner M., Regal, C. A., Jin, D. S. *Nature* **426** (2003) 537
- [85] Perali A., Pieri P., Pisani L., Strinati G. C., *Phys. Rev. Lett.* **92** (2004) 220404
- [86] Yildirim T., et al., *Physical Review Letters* **87** (2001) 037001
- [87] Boeri L., Cappelluti E., Pietronero L., *Physical Review B* **71** (2005) 012501